Preparation and Characterization of Cobaltaboranes Containing Cobalt Carbonyl Fragments

Chang-Soo Jun,[†] Jean-François Halet,*[,‡] Arnold L. Rheingold,*[,§] and Thomas P. Fehlner*[,†]

Department of Chemistry and Biochemistry, University of Notre Dame, Notre Dame, Indiana 46556, Department of Chemistry and Biochemistry, University of Delaware, Newark, Delaware 19716, and Laboratoire de Chimie du Solide et Inorganique Moléculaire, URA CNRS 1495, Université de Rennes 1, Avenue du Général Leclerc, 35042 Rennes Cedex, France

Received November 8, 1994[⊗]

Two new metallacarboranes, $Co_2(CO)_6B_2H_4$ and $Co_5(CO)_{13}(\mu\text{-}CO)B_2H$, have been prepared in low yield by the reaction of $BH_3{\cdot}SMe_2$ with $Co_2(CO)_8$. The former has been fully characterized spectroscopically and is isoelectronic with $Fe_2(CO)_6B_2H_6$, on the one hand, and $Co_2(CO)_6C_2H_2$, on the other. The latter has been characterized both by spectroscopy and by a single-crystal X-ray diffraction study (orthorhombic *Pna*2, $a = 24.886(4)$ Å, $b = 9.846(5)$ Å, $c = 9.248(3)$ Å, $V = 2266.3(9)$ Å^3, d(calc) = 2.076 g/cm^3, $Z = 4$). The structure exhibited by $Co_5(CO)_{13}(\mu\text{-}CO)B_2H$ is unusual, and aspects of its electronic structure have been elucidated by molecular orbital calculations. Mechanistic studies suggest solvent-free $(CO)_4CoBH_2$ as an intermediate and suggest that the formation of the new compounds constitutes an example of B−H, Co−Co σ-bond metathesis.

Introduction

Although there are numerous metallaboranes containing η^5-C_5H_5Co or $Fe(CO)_3$ fragments (both isolobal with BH),[1−5] there are only a few reports of metallaboranes containing the η^5-C_5H_5-Ni[6−10] or $Co(CO)_3$ fragments[11−14] (both isolobal with CH). Two-electron fragments are ideal for the formal construction of clusters analogous to polyhedral borane cages, and the inclusion of three-electron fragments would permit the like construction of clusters analogous to polyhedral carboranes.[15] Thus, the scarcity of metallaborane clusters containing three-electron fragments, e.g., cobalt tricarbonyl fragments, presents a significant synthetic challenge.

The synthesis of main group−transition element clusters isoelectronic with organometallic complexes provides more than an exercise of the isolobal analogy. Both isolobal analogies and cluster electron-counting protocols are now firmly established as conceptual, as well as practical, tools of the modern chemist. Indeed clusters exhibiting nonconforming geometries are viewed with more interest than they might be otherwise. Yet, even when the rules are followed precisely, neither analogous fragments nor analogous clusters are the same chemically speaking. Hence, the synthesis of main group element analogs also provides an experimental platform for developing an understanding of the role of element variation in both structure and reactivity.[16] In other words, the importance of the number and population of the frontier orbitals of a fragment in defining structural behavior is well accepted whereas the importance of these, and other factors such as frontier orbital energies, in the control of chemistry is not as well appreciated.

Chart 1

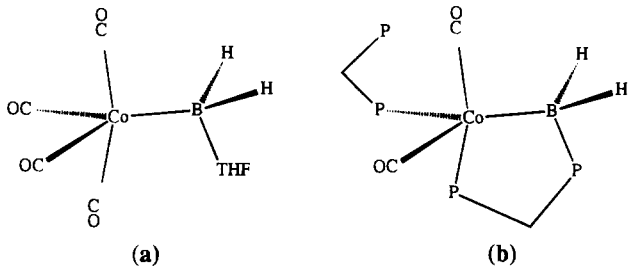

We have already investigated the reaction of $BH_3{\cdot}THF$ with $Co_2(CO)_8$ and demonstrated the formation of $(CO)_4CoBH_2{\cdot}THF$ at low temperatures (Chart 1a).[17] Subsequently, a phosphine analog of this compound, $[(CO)_2(\eta^1\text{-dppm})Co(\mu\text{-dppm})BH_2$, was isolated and characterized by Elliot et al (Chart 1b)[18] supporting the proposed structure of the former compound which contains an unsupported Co−B bond. Although $(CO)_4CoBH_2{\cdot}THF$ was found of no value for the construction of larger cobaltaboranes due to ready reaction with THF above 0 °C, it does provide an example of a similarity between the reactivity of Si-H bonds[19] and B−H bonds as shown in reactions1 and 2. As the utilization

$$2R_3SiH + Co_2(CO)_8 \rightarrow 2(CO)_4CoSiR_3 + H_2 \quad (1)$$

$$2BH_3{\cdot}THF + Co_2(CO)_8 \rightarrow 2(CO)_4CoBH_2{\cdot}THF + H_2 \quad (2)$$

of B−H bonds to form B−Co bonds is still an attractive cluster-building route, we have now revisited this system completely

[†] University of Notre Dame.
[‡] Université de Rennes.
[§] University of Delaware.
[⊗] Abstract published in *Advance ACS Abstracts,* March 15, 1995.

(1) Housecroft, C. E.; Fehlner, T. P. *Adv. Organomet. Chem.* **1982**, *21*, 57.
(2) Housecroft, C. E. In *Inorganometallic Chemistry*; Fehlner, T. P. , Ed.; Plenum Press: New York, 1992; p 73.
(3) Kennedy, J. D. *Prog. Inorg. Chem.* **1984**, *32*, 519.
(4) Kennedy, J. D. *Prog. Inorg. Chem.* **1986**, *34*, 211.
(5) Grimes, R. N. In *Metal Interactions with Boron Clusters*; Grimes, R. N., Ed.; Plenum: New York, 1982; p 269.
(6) Bowser, J. R.; Grimes, R. N. *J. Am. Chem. Soc.* **1978**, *100*, 4623.
(7) Bowser, J. R.; Bonny, A.; Pipal, J. R.; Grimes, R. N. *J. Am. Chem. Soc.* **1979**, *101*, 6229.
(8) Leyden, R. N.; Hawthorne, M. F. *J. Chem. Soc., Chem. Commun.* **1975**, 310.
(9) Sullivan, B. P.; Leyden, R. N.; Hawthorne, M. F. *J. Am. Chem. Soc.* **1975**, *97*, 456.
(10) Leyden, R. N.; Sullivan, B. P.; Baker, R. T.; Hawthorne, M. F. *J. Am. Chem. Soc.* **1978**, *100*, 3758.
(11) Sneath, R. L.; Little, J. L.; Burke, A. R.; Todd, L. *J. Chem. Soc., Chem. Commun.* **1970**, 693.
(12) Schmid, G.; Bätzel, V.; Etzrodt, G.; Pfeil, R. *J. Organomet. Chem.* **1975**, *86*, 257.
(13) Shore, S. G.; Ragaini, J.; Schmitkons, T.; Barton, L.; Medford, G.; Plotkin, J. *Abstr. IMEBORON* **1979**, *4*, 36.
(14) Schubert, D. M.; Knobler, C. B.; Wegner, P. A.; Hawthorne, M. F. *J. Am. Chem. Soc.* **1988**, *110*, 5219.
(15) Mingos, D. M. P.; Wales, D. J. *Introduction to Cluster Chemistry*; Prentice Hall: New York, 1990.

0020-1669/95/1334-2101$09.00/0

eliminating the presence of THF. Some preliminary results of this work have already appeared.[20]

Experimental Section

General Procedures. All manipulations were carried out under an atmosphere of argon or in a standard vacuum line using Schlenk techniques. Analytical grade solvents and deuterated solvents were properly dried, degassed, and freshly distilled before use. Spectra were recorded on the following instruments: IR, Nicolet 205 FTIR, using a 0.2 mm cell provided with NaCl windows; ^{1}H NMR, Varian 500 MHz or GN 300 MHz spectrometers using residual solvent as reference; ^{11}B NMR, Nicolet 300 MHz spectrometer operating at 96 MHz using $B_3H_8N(Me)_4$ ($\delta = -29.7$ ppm) in acetone-d_6 as internal reference; FAB MS, JEOL JMS-AX505HA spectrometer with a *p*-nitrobenzyl alcohol matrix and Xe atoms. The following reagents were used as received without further purification, unless otherwise mentioned: $BH_3{\cdot}SMe_2$ and SEt_2 (Aldrich), $Co_2(CO)_8$ (Strem, recrystallization from hexane), 60−200 mesh silica gel ("Baker Analyzed" dried in an oven at 100 °C at least overnight).

A 250 mL two-neck round-bottom flask into which was weighed 3.0 g (8.8 mmol) of $Co_2(CO)_8$ was equipped with a stirring bar and a condenser. Under 1 atm of CO (*Cautionary note*: This reaction must be carried out in a functioning hood as CO gas is odorless and toxic.) 10 mL of toluene and 4.4 mmol of $BH_3{\cdot}SMe_2$ were introduced. Then the reaction flask was immersed in a 75 °C water bath and the reaction mixture stirred for 15 min. The hot bath was replaced by an ice bath, causing the precipitation of a purple-brown crystalline solid not containing boron (mainly $Co_4(CO)_{12}$). After 30 min, the solution was decanted into a 40 mm o.d. schlenk tube. The toluene was removed under vacuum until the appearance of yellow-orange compounds in the liquid nitrogen trap. The ^{11}B NMR spectrum of the remaining material showed the presence of several boron-containing products. As described below, two of these have been isolated and characterized. The others did not survive column chromatography even at −70 °C, and attempts at fractional crystallization have been frustrated by the presence of $Co_4(CO)_{12}$ and the high sensitivity of the products.

$Co_2(CO)_6B_2H_4$. The reaction mixture was first fractionated under vacuum, and the volatile red-orange material passing 0 °C was identified as $Co_2(CO)_6B_2H_4$. It is an extremely air-sensitive liquid at room temperature, and it decomposes under nitrogen at room temperature within 2 days. The isolated yield was 6% (0.1 mmol by ^{11}B NMR) based on initial boron. Note that although $Co_2(CO)_8$ was in excess and was totally consumed, some of the $BH_3{\cdot}SMe_2$ remained unreacted. In the absence of CO gas, yields were lower (2%) and the $Co_2(CO)_8$ was even more rapidly consumed. MS/EI, P^+ *m/e*: 312, 2 borons, −6CO, calcd for $^{12}C_6{}^1H_4{}^{16}O_6{}^{11}B_2{}^{59}Co_2$ 311.885 79, obsd 311.8860. IR (hexane, cm^{-1}) 2584 vw, 2523 vw, 2102 ms, 2061 s, 2047 s, 2034 s, 2015 s. NMR: ^{11}B (hexane, 22 °C, δ) −0.9 br d, $J_{BH} = 130$ Hz, {^{1}H} br s, fwhm 100 Hz; ^{1}H (toluene-d_8, 22 °C, δ) 3.3 br 2H, −0.6 br 1H, −13.7 br 1H.

$Co_5(CO)_{13}(\mu$-CO)B_2H. The residue from the fractionation was dissolved in 20 mL of hexane, and the solution was cooled to −4 °C overnight to precipitate additional non-boron-containing compounds. The residues from four reactions, treated in like manner, were combined and repeatedly crystallized until the total volume was ≈5 mL. The hexane solution of the products was loaded on a −20 °C silica gel column (2 × 12 cm), and the second band (greenish brown, $R_f = 0.45$) eluted with hexanes was identified as $Co_5(CO)_{13}(\mu$-CO)B_2H. Deep brown, moderately air-sensitive crystals formed overnight in hexane at −4 °C. The isolated yield was 0.4% (0.02 mmol) based on boron. We later found that $Co_5(CO)_{13}(\mu$-CO)B_2H can be isolated in 10% yield from the reaction of $Fe_2(CO)_6B_2H_6$ with $Co_2(CO)_8$, in which the primary product (45%) is $FeCo(CO)_6B_2H_5$.[21] MS/FAB, $P^+ - CO$ 682, 2 borons, −10CO, calcd for $^{12}C_{13}{}^1H_1{}^{16}O^{[31]1}B_2{}^{59}Co_5$ 681.63, obsd 681.58. EI, P^+ *m/e* 710, 2 borons, −14 CO. IR (hexane, cm^{-1}): 2511 vw (BH); 2107 vw, 2070 s, 2062 vs, 2044 s, 2034 m, 2026 sh, 1990 vw, 1976 w, 1867 m, 1735 vw (CO). NMR: ^{11}B (hexane, 22 °C, δ) 150.4, br s, fwhm 140 Hz; {^{1}H} br s, fwhm 140 Hz, 74, d, $J_{BH} = 144$ Hz; ^{1}H (toluene-d_8, δ) 22 °C, 9.5 br, apparent d, 60 °C, 9.5 q.

$Co_5(CO)_{13}(\mu$-CO)B_2H crystallizes in the orthorhombic space group *Pna*2, with $a = 24.886(4)$ Å, $b = 9.846(5)$ Å, $c = 9.248(3)$ Å, $V = 2266.3(9)$ Å^3, d(calc) = 2.076 g/cm^3, $Z = 4$. Of 1588 data collected ($2\Theta_{max} = 45°$, Siemens P4, 239 K), 1103 were observed at $4\sigma(F_o)$. Although $Co_5(CO)_{13}(\mu$-CO)B_2H possesses an approximate mirror plane defined by B(1), B(2), and Co(5), it does not coincide with the crystallographic *c* axis; thus the noncentrosymmetric space group is required. The data were corrected for absorption. Limitations in data restricted anisotropic refinement to the Co atoms. $R(F) = 5.94\%$, $R_w(F) = 5.89\%$. A Rogers test was used to determine the preference for the hand reported. Coordinates and selected bond distances and angles are given in Tables 1 and 2, respectively. Other data were deposited in conjunction with the original communication.[20]

MO Calculations. Molecular orbital (MO) calculations were carried out within the extended Hückel formalism[22] using the weighted *H* formula.[23] The standard atomic parameters utilized were taken from the literature. The exponents (ζ) and the valence shell ionization potentials (H_{ii} in eV) were respectively as follows: 1.3, −13.6 for H 1s; 1.3, −15.2 for B 2s; 1.3, −8.5 for B 2p; 1.625, −21.4 for C 2s; 1.625, −11.4 for C 2p; 2.275, −32.3 for O 2s; 2.275, −14.8 for O 2p; 2.0, −9.21 for Co 4s; 2.0, −5.29 for Co 4p. The H_{ii} for Co 3d was set

Table 1. Atomic Coordinates ($\times 10^4$) and Equivalent Isotropic Displacement Coefficients (Å^2 × 10^3) for $Co_5(CO)_{13}(\mu$-CO)B_2H

	x	*y*	*z*	*U*(eq)
Co(1)	1250(1)	4281(3)	5000	39(1)
Co(2)	585(1)	2481(3)	6356(6)	41(1)
Co(3)	1151(1)	349(3)	5799(4)	40 (1)
Co(4)	1858(1)	1998(3)	4386(5)	41(1)
Co(5)	1373(1)	1845(3)	7905(5)	41(1)
B(1)	1397(10)	2488(27)	5974(32)	36(6)
B(2)	1026(11)	2212(26)	4370(36)	42(7)
O(1)	2187(8)	5797(19)	6028(26)	84(6)
O(2)	950(9)	5216(25)	2273(32)	106(8)
O(3)	509(7)	6097(18)	6495(23)	67(5)
O(4)	-380(10)	2933(22)	4663(28)	96(7)
O(5)	154(9)	3573(22)	8924(27)	99(8)
O(6)	142(8)	−296(22)	7211(25)	90(7)
O(7)	792(7)	−1441(8)	3509(26)	69(5)
O(8)	1557(8)	−1977(21)	7535(24)	80(6)
O(9)	2232(9)	−983(23)	4185(27)	101(7)
O(10)	1854(11)	2665(28)	1480(44)	135(10)
O(11)	2894(9)	3058(21)	5432(25)	87(6)
O(12)	920(11)	295(27)	10269(32)	122(9)
O(13)	1530(8)	4741(22)	8971(24)	83(6)
O(14)	2496(8)	931(20)	7881(25)	83(6)
C(1)	1813(9)	5263(25)	5590(30)	47(6)
C(2)	1104(12)	4897(31)	3316(37)	72(9)
C(3)	762(10)	5318(26)	5930(33)	55(7)
C(4)	32(13)	2747(31)	5350(35)	78(9)
C(5)	318(10)	3068(27)	7921(36)	58(7)
C(6)	478(12)	472(27)	6671(35)	67(8)
C(7)	911(10)	−721(25)	4420(32)	50(7)
C(8)	1389(13)	−1034(33)	6859(39)	75(9)
C(9)	2047(10)	203(28)	4324(34)	63(8)
C(10)	1859(14)	2379(35)	2662(46)	93(11)
C(11)	2465(11)	2618(25)	5030(32)	56(7)
C(12)	1109(14)	876(33)	9266(44)	90(10)
C(13)	1446(10)	3566(27)	8588(30)	52(7)
C(14)	2065(10)	1314(23)	7962(31)	49(7)

[a] Equivalent isotropic *U* defined as one-third of the trace of the orthogonalized U_{ij} tensor.

(16) Fehlner, T. P., Ed. *Inorganometallic Chemistry*; Plenum: New York, 1992.
(17) Basil, J. D.; Aradi, A. A.; Bhattacharyya, N. K.; Rath, N. P.; Eigenbrot, C.; Fehlner, T. P. *Inorg. Chem.* **1990**, *29*, 1260.
(18) Elliot, D. J.; Levy, C. J.; Puddephatt, R. J.; Holah, D. G.; Hughes, A. N.; Magnuson, V. R.; Moser, I. M. *Inorg. Chem.* **1990**, *29*, 5014.
(19) Chalk, A. J.; Harrod, J. F. *J. Am. Chem. Soc.* **1967**, *89*, 1640.
(20) Jun, C.-S.; Fehlner, T. P.; Rheingold, A. L. *J. Am. Chem. Soc.* **1993**, *115*, 4393.
(21) Jun, C.-S.; Fehlner, T. P. *Organometallics* **1994**, *13*, 2145.
(22) Hoffmann, R. *J. Chem. Phys.* **1963**, *39*, 1397.
(23) Ammeter, J. H.; Bürgi, H.-D.; Thibeault, J. C.; Hoffmann, R. *J. Am. Chem. Soc.* **1978**, *100*, 3686.

Table 2. Selected Bond Lengths (Å) and Angles (deg) for $Co_5(CO)_{13}(\mu\text{-}CO)B_2H$

Co(1)−Co(2)	2.700(5)	Co(1)−Co(4)	2.668(4)	Co(4)−C(10)	1.734(45)	Co(4)−C(11)	1.736(28)
Co(1)−B(1)	1.951(26)	Co(1)−B(2)	2.087(26)	Co(5)−B(1)	1.993(31)	Co(5)−C(12)	1.741(39)
Co(1)−C(1)	1.769(24)	Co(1)−C(2)	1.790(36)	Co(5)−C(13)	1.737(26)	Co(5)−C(14)	1.793(24)
Co(1)−C(3)	1.798(27)	Co(2)−Co(3)	2.484(4)	B(1)−B(2)	1.847(45)	O(1)−C(1)	1.138(32)
Co(2)−Co(5)	2.553(6)	Co(2)−B(1)	2.056(27)	O(2)−C(2)	1.135(47)	O(3)−C(3)	1.106(33)
Co(2)−B(2)	2.257(34)	Co(2)−C(4)	1.713(34)	O(4)−C(4)	1.241(42)	O(5)−C(5)	1.166(42)
Co(2)−C(5)	1.764(34)	Co(2)−C(6)	1.903(26)	O(6)−C(6)	1.221(36)	O(7)−C(7)	1.155(36)
Co(3)−Co(4)	2.714(5)	Co(3)−Co(5)	2.553(6)	O(8)−C(8)	1.174(39)	O(9)−C(9)	1.198(34)
Co(3)−B(1)	2.078(25)	Co(3)−B(2)	2.246(29)	O(10)−C(10)	1.194(62)	O(11)−C(11)	1.208(36)
Co(3)−C(6)	1.884(30)	Co(3)−C(7)	1.783(29)	O(12)−C(12)	1.218(50)	O(13)−C(13)	1.169(33)
Co(3)−C(8)	1.755(33)	Co(4)−B(1)	1.992(29)	O(14)−C(14)	1.131(31)		
Co(4)−B(2)	2.081(28)	Co(4)−C(9)	1.726(26)				

Co(2)−Co(1)−Co(4)	88.4(1)	Co(2)−Co(1)−B(1)	49.3(8)	Co(1)−Co(4)−B(1)	46.8(8)	Co(3)−Co(4)−B(1)	49.5(7)
Co(4)−Co(1)−B(1)	48.1(9)	Co(2)−Co(1)−B(2)	54.4(9)	Co(1)−Co(4)−B(2)	50.3(7)	Co(3)−Co(4)−B(2)	53.9(8)
Co(4)−Co(1)−B(2)	50.1(8)	B(1)−Co(1)−B(2)	54.3(12)	B(1)−Co(4)−B(2)	53.9(13)	Co(1)−Co(4)−C(9)	157.5(10)
Co(2)−Co(1)−C(1)	129.8(9)	Co(4)−Co(1)−C(1)	91.7(8)	Co(3)−Co(4)−C(9)	69.8(10)	B(1)−Co(4)−C(9)	113.8(13)
B(1)−Co(1)−C(1)	97.2(11)	B(2)−Co(1)−C(1)	141.2(11)	B(2)−Co(4)−C(9)	111.3(11)	Co(1)−Co(4)−C(10)	93.5(11)
Co(2)−Co(1)−C(2)	122.0(10)	Co(4)−Co(1)−C(2)	99.0(10)	Co(3)−Co(4)−C(10)	128.0(11)	B(1)−Co(4)−C(10)	136.3(14)
B(1)−Co(1)−C(2)	139.8(13)	B(2)−Co(1)−C(2)	87.8(13)	B(2)−Co(4)−C(10)	88.5(15)	C(9)−Co(4)−C(10)	99.2(16)
C(1)−Co(1)−C(2)	107.5(13)	Co(2)−Co(1)−C(3)	70.3(8)	Co(1)−Co(4)−C(11)	98.6(8)	Co(3)−Co(4)−C(11)	124.3(10)
Co(4)−Co(1)−C(3)	157.1(9)	B(1)−Co(1)−C(3)	109.3(12)	B(1)−Co(4)−C(11)	98.1(13)	B(2)−Co(4)−C(11)	146.9(12)
B(2)−Co(1)−C(3)	117.4(11)	C(1)−Co(1)−C(3)	95.4(12)	C(9)−Co(4)−C(11)	95.3(12)	C(10)−C(4)−C(11)	106.9(15)
C(2)−Co(1)−C(3)	99.5(14)	Co(1)−Co(2)−Co(3)	91.9(2)	Co(2)−Co(5)−Co(3)	58.2(1)	Co(2)−Co(5)−B(1)	52.0(8)
Co(1)−Co(2)−Co(5)	88.1(1)	Co(3)−Co(2)−Co(5)	60.9(1)	Co(3)−Co(5)−B(1)	52.7(7)	Co(2)−Co(5)−C(12)	106.8(12)
Co(1)−Co(2)−B(1)	46.0(7)	Co(3)−Co(2)−B(1)	53.5(7)	Co(3)−Co(5)−C(12)	105.3(12)	B(1)−Co(5)−C(12)	154.1(15)
Co(5)−Co(2)−B(1)	49.8(9)	Co(1)−Co(2)−B(2)	48.8(6)	Co(2)−Co(5)−C(13)	95.8(9)	Co(3)−Co(5)−C(13)	146.4(10)
Co(3)−Co(2)−B(2)	56.3(7)	Co(5)−Co(2)−B(2)	96.8(8)	B(1)−Co(5)−C(13)	95.3(12)	C(12)−Co(5)−C(13)	102.3(15)
B(1)−Co(2)−B(2)	50.4(11)	Co(1)−Co(2)−C(4)	96.7(11)	Co(2)−Co(5)−C(14)	145.1(10)	Co(3)−Co(5)−C(14)	94.9(9)
Co(3)−Co(2)−C(4)	116.2(11)	Co(5)−Co(2)−C(4)	174.5(10)	B(1)−Co(5)−C(14)	94.7(12)	C(12)−Co(5)−C(14)	101.4(14)
B(1)−Co(2)−C(4)	133.1(14)	B(2)−Co(2)−C(4)	84.6(14)	C(13)−Co(5)−C(14)	97.9(11)	Co(1)−B(1)−Co(2)	84.7(10)
Co(1)−Co(2)−C(5)	118.3(8)	Co(3)−Co(2)−C(5)	130.6(9)	Co(1)−B(1)−Co(3)	135.5(15)	Co(2)−B(1)−Co(3)	73.9(9)
Co(5)−Co(2)−C(5)	80.7(9)	B(1)−Co(2)−C(5)	122.0(12)	Co(1)−B(1)−Co(4)	85.2(12)	Co(2)−B(1)−Co(4)	135.2(15)
B(2)−Co(2)−C(5)	167.1(10)	C(4)−Co(2)−C(5)	99.1(14)	Co(3)−B(1)−Co(4)	83.6(10)	Co(1)−B(1)−Co(5)	135.8(15)
Co(1)−Co(2)−C(6)	140.2(9)	Co(3)−Co(2)−C(6)	48.7(9)	Co(2)−B(1)−Co(5)	78.1(10)	Co(3)−B(1)−Co(5)	77.6(10)
Co(5)−Co(2)−C(6)	77.6(9)	B(1)−Co(2)−C(6)	99.8(11)	Co(4)−B(1)−Co(5)	134.3(14)	Co(1)−B(1)−B(2)	66.6(12)
B(2)−Co(2)−C(6)	95.8(12)	C(4)−Co(2)−C(6)	97.0(14)	Co(2)−B(1)−B(2)	70.4(13)	Co(3)−B(1)−B(2)	69.5(12)
C(5)−Co(2)−C(6)	96.1(13)	Co(2)−Co(3)−Co(4)	92.0(1)	Co(4)−B(1)−B(2)	65.5(14)	Co(5)−B(1)−B(2)	139.4(17)
Co(2)−Co(3)−Co(5)	60.9(2)	Co(4)−Co(3)−Co(5)	88.3(2)	Co(1)−B(2)−Co(2)	76.8(10)	Co(1)−B(2)−Co(3)	118.7(16)
Co(2)−Co(3)−B(1)	52.7(7)	Co(4)−Co(3)−B(1)	46.8(8)	Co(2)−B(2)−Co(3)	67.0(9)	Co(1)−B(2)−Co(4)	79.6(10)
Co(5)−Co(3)−B(1)	49.7(9)	Co(2)−Co(3)−B(2)	56.7(8)	Co(2)−B(2)−Co(4)	119.2(15)	Co(3)−B(2)−Co(4)	77.6(10)
Co(4)−Co(3)−B(2)	48.5(7)	Co(5)−Co(3)−B(2)	97.1(8)	Co(1)−B(2)−B(1)	59.1(11)	Co(2)−B(2)−B(1)	59.1(13)
B(1)−Co(3)−B(2)	50.4(11)	Co(2)−Co(3)−C(6)	49.3(8)	Co(3)−B(2)−B(1)	60.1(12)	Co(4)−B(2)−B(1)	60.6(12)
Co(4)−Co(3)−C(6)	140.9(8)	Co(5)−Co(3)−C(6)	77.9(10)	Co(1)−C(1)−O(1)	174.5(24)	Co(1)−C(2)−O(2)	171.5(26)
B(1)−Co(3)−C(6)	99.6(11)	B(2)−Co(3)−C(6)	96.7(12)	Co(1)−C(3)−O(3)	170.8(23)	Co(2)−C(4)−O(4)	177.6(31)
Co(2)−CO(3)−C(7)	114.8(8)	Co(4)−Co(3)−C(7)	98.0(9)	Co(2)−C(5)−O(5)	174.2(24)	Co(2)−C(6)−Co(3)	82.0(11)
Co(5)−Co(3)−C(7)	172.6(9)	B(1)−Co(3)−C(7)	133.6(12)	Co(2)−C(6)−O(6)	137.3(23)	Co(3)−C(6)−O(6)	140.7(21)
B(2)−Co(3)−C(7)	84.4(11)	C(6)−Co(3)−C(7)	94.8(13)	Co(3)−C(7)−O(7)	175.3(22)	Co(3)−C(8)−O(8)	178.0(25)
Co(2)−Co(3)−C(8)	129.7(12)	Co(4)−Co(3)−C(8)	119.7(11)	Co(4)−C(9)−O(9)	171.7(25)	Co(4)−C(10)−O(10)	178.7(31)
Co(5)−Co(3)−C(8)	80.7(12)	B(1)−Co(3)−C(8)	123.0(14)	Co(4)−C(11)−O(11)	177.7(26)	Co(5)−C(12)−O(12)	175.2(31)
B(2)−Co(3)−C(8)	168.1(13)	C(6)−Co(3)−C(8)	94.2(14)	Co(5)−C(13)−O(13)	174.3(24)	Co(5)−C(14)−O(14)	173.6(26)
C(7)−Co(3)−C(8)	99.3(14)	Co(1)−Co(4)−Co(3)	87.7(1)				

equal to −13.18. A linear combination of two Slater-type orbitals of exponents $\zeta_1 = 5.55$, $\zeta_2 = 1.90$ with weighting coefficients $c_1 = 0.5551$, $c_2 = 0.6461$ was used to represent the 3d atomic orbitals (AO) of Co. An idealized structure of $Co_5(CO)_{13}(\mu\text{-}CO)B_2H$ (of C_s symmetry), derived from the crystal data, was used for the calculations. The following bond distances (Å) were used; Co−Co = 2.65; Co(basal)−B = 2.09; Co(capping)−B = 1.99; Co−C(O) = 1.75; C−O = 1.15; B−H = 1.20.

Results and Discussion

New Cobaltaboranes. Although $Co_2(CO)_6B_2H_4$ has not been crystallographically characterized, its structure is clearly revealed by the spectroscopic data. The ^{11}B NMR spectrum exhibits a single broad doublet at δ −0.9 with a B−H coupling corresponding to a terminal B−H. The ^1H NMR spectrum exhibits three broad signals at δ 3.3, −0.6, and −13.7 in the intensity ratio of 2:1:1 that thermally decouple at lower temperatures. These are assigned to B−H terminal, B−H−B bridge, and B−H−Co edge- or face-bridging protons, respectively. The infrared spectrum of $Co_2(CO)_6B_2H_4$ shows two terminal B−H stretches, indicating asymmetric boron atom environments or coupled B−H vibrations. There are five strong CO stretches observed.

Three structures, which are consistent with the spectroscopic data, are shown in Figure 1. They differ only in the placement of the B−H−Co bridging hydrogen.

Compounds containing hydrogen atoms either bridging a BCoCo face or Co−B edge are known, and the chemical shift observed here (−13.7 ppm) does not permit a definitive choice between them.[5,24−26] The infrared data in the carbonyl stretching region are suggestive. Whereas a molecule with a $M_2(CO)_6$ "sawhorse" fragment usually exhibits only three or four stretching vibrations, even without formal C_{2v} symmetry,[27] $Co_2(CO)_6B_2H_4$ exhibits five. This observation favors structures

(24) Miller, V. R.; Weiss, R.; Grimes, R. N. *J. Am. Chem. Soc.* **1977**, *99*, 5646.
(25) Feilong, J.; Fehlner, T. P.; Rheingold, A. L. *J. Am. Chem. Soc.* **1987**, *109*, 1860.
(26) Feilong, J.; Fehlner, T. P.; Rheingold, A. L. *J. Organomet. Chem.* **1988**, *348*, C22.

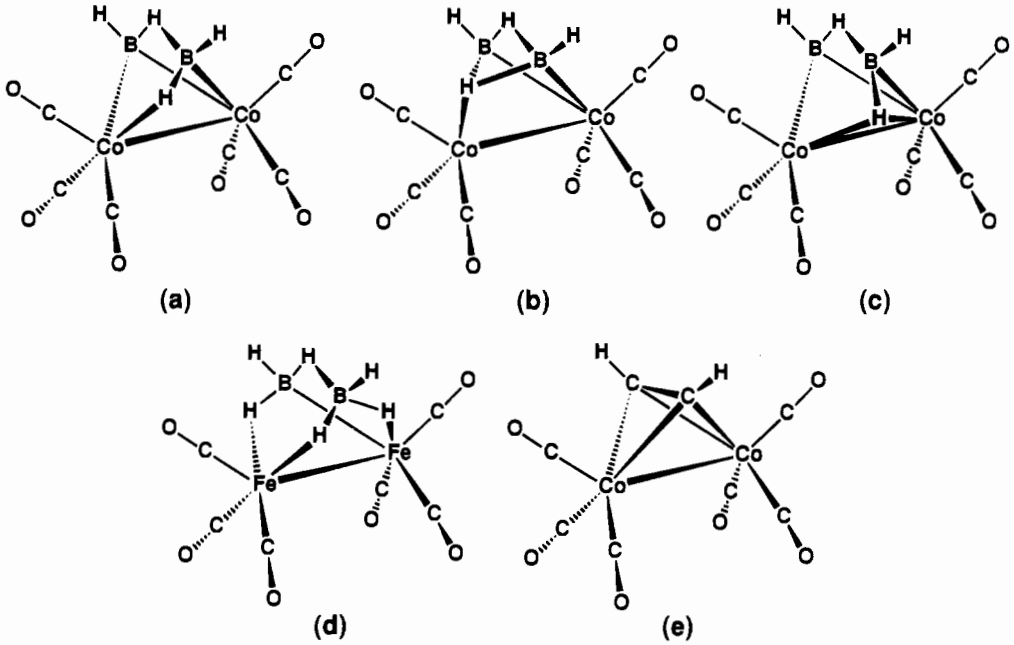

Figure 1. Postulated structures for $Co_2(CO)_6B_2H_4$ (a–c) and known structures for $Fe_2(CO)_6B_2H_6$ and $Co_2(CO)_6C_2H_2$.

a and **b** as the cobalt centers have distinctly different ligand environments. Likewise, if the two B–H stretches observed are due to different B–H bonds, then structure **a** is favored over **b**. Although we favor a structure with an edge-bridging hydrogen, one with a face-bridging hydrogen cannot be ruled out.

The new metallaborane is isoelectronic with $B_2H_6Fe_2(CO)_6$ (**d**).[28] The postulated structure of the ferraborane is corroborated by a structure determination on the dimer[29] as well as a structure determination on a related tantalum compound.[30] The new cobaltaborane is also isoelectronic with $C_2H_2Co_2(CO)_6$ (**e**).

We previously characterized the complex fluxional behavior of the hydrogens of $Fe_2(CO)_6B_2H_6$, and related fluxional behavior is observed for $Co_2(CO)_6B_2H_4$ by ^1H NMR. All three proton signals are observed between −90 and +22 °C but at 60 °C the signals at δ 3.3 and −13.7 merge with the baseline. At 75 °C the δ −0.6 signal is largely lost . The 22 °C spectrum is recovered on reducing the temperature, showing that no decomposition had occurred. Spin saturation transfer experiments at 25 °C show that the rate constant for the δ 3.3 and −13.7 proton exchange is 1.6 s^{-1} whereas for exchange of the δ 3.3 or −13.7 protons with the δ −0.6 proton it is 1.2 s^{-1}. These NMR data require three distinct fluxional processes. The first distributes the Co–H–B proton over the Co–B edges/faces, the second exchanges the Co–H–B and B–H terminal protons, and the third exchanges B–H–B protons with the rest. The differences between the rates of the fluxional processes of $Fe_2(CO)_6B_2H_6$ and $Co_2(CO)_6B_2H_4$ are striking. Despite having fewer hydrogens (and therefore more potential sites for placing them), the H interchange in $Co_2(CO)_6B_2H_4$ is much slower than it is in $Fe_2(CO)_6B_2H_6$,

Although $Co_5(CO)_{13}(\mu\text{-CO})B_2H$ has been crystallographically characterized in the solid state, the hydrogen atom was not located and the spectroscopic data are necessary in order to fully characterize the molecule. To begin, consider the molecular structure derived from the solid state structure shown in Figure

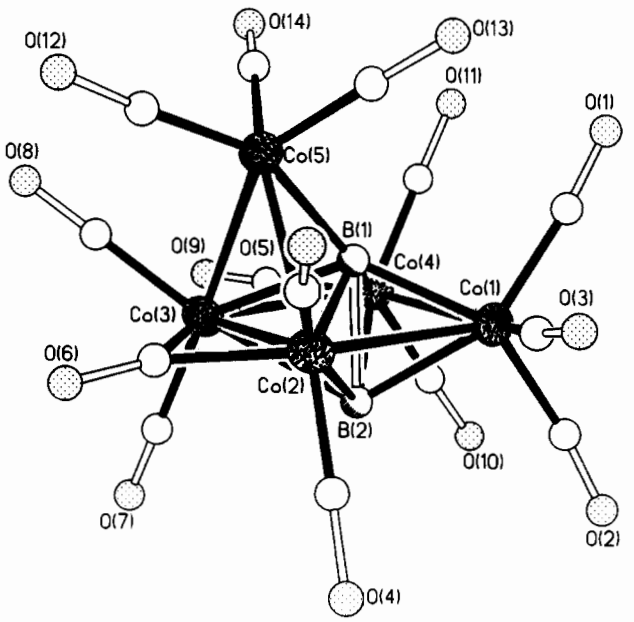

Figure 2. Molecular structure of $Co_5(CO)_{13}(\mu\text{-CO})B_2H$ established by X-ray diffraction.

2. In terms of geometry, the core structure is most easily described as a trans Co_4B_2 octahedron with a Co atom capping a Co_2B triangular face. Three of the cobalt atoms have three CO ligands, and the other two have two. There is one bridging carbonyl to complete the structure. Bond distances and angles are within the expected ranges, but the variations in similar bond types are considered further below.

No parent ion was observed in the original FAB mass spectrum; however, later EI data showed a weak parent ion consistent with the molecular formula found in the solid state. The infrared spectrum confirms the presence of a bridging CO ligand as well as a terminal B–H. The ^{11}B NMR shows two types of boron atoms in very different environments. One, at very low field (δ 150), shows no coupling to hydrogen whereas the other (δ 74) shows coupling to a terminal proton (J_{BH} = 144 Hz). In the ^1H NMR spectrum, a single resonance is observed in the terminal region (δ 9.5). These data allow the position of the hydrogen atom to be unambiguously placed in

(27) Bor, G. *J. Organomet. Chem.* **1975**, *91*, 181.
(28) Jacobsen, G. B.; Andersen, E. L.; Housecroft, C. E.; Hong, F.-E.; Buhl, M. L.; Long, G. J.; Fehlner, T. P. *Inorg. Chem.* **1987**, *26*, 4040.
(29) Jun, C.-S.; Powell, D. R.; Haller, K. J.; Fehlner, T. P. *Inorg. Chem.* **1993**, *32*, 5071.
(30) Ting, C.; Messerle, L. *J. Am. Chem. Soc.* **1989**, *111*, 3449.

the structure. First, the lower field chemical shift will be associated with the position involving the greater number of direct metal−boron interactions, i.e., B_1.[31,32] Second, the boron atom B_2 can accommodate a terminal hydrogen atom, whereas if there were a hydrogen attached to B_1, it would almost certainly be B−H−Co bridging as the site is similar to that in $HFe_4(CO)_{12}BH_2$.[33] Both the magnitude of the observed B−H coupling and the value of the ^1H chemical shift rule out the presence of such a bridging hydrogen.

Geometric and Electronic Structure of $Co_5(CO)_{13}(\mu$-CO)B_2H. The structure of $Co_5(CO)_{13}(\mu$-CO)B_2H is a rather unusual one[34] and deserves additional discussion. The geometric parameters defining the structure provide the first source of information on the nature of the bonding. The B−B distance is 1.85(4) Å, which is within the range observed for polyhedral boranes with B−B bonding.[35] The Co−Co and Co−B distances fall within ranges that can be associated with bonding but can be divided into sets of short and long distances. That is, all of the metal interactions with B(1) plus those between Co(1) and Co(4) with B(2) are similar; d(CoB(av)) = 2.03(3) Å. The two other metal interactions with B(2) are longer; d(CoB(av)) = 2.26(3) Å. The three Co−Co distances in the triangle made up by Co(2), Co(3), and Co(5) are short (d(CoCo(av)) = 2.53(1) Å), whereas the other three Co−Co edges (Co(1)−Co(2), Co(1)−Co(4), Co(3)−Co(4)) are long (d(CoCo(av)) = 2.69(1) Å).

In our preliminary communication, we suggested one way of accommodating both the cluster composition (that is, polyhedral electron count, pec)[35,36] and geometry with existing cluster structure concepts. $Co_5(CO)_{13}(\mu$-CO)B_2H has a pec of 80, which is the proper count for a trigonal prismatic $M_6(B)$ boride cluster (Chart 2a)[37] in which one metal vertex has been replaced by a BH fragment, i.e., 90 − 10 = 80 (Chart 2b). In such a cluster, the axial distances are expected to be longer than the metal−metal distances in the triangular faces. The observed structure of $Co_5(CO)_{13}(\mu$-CO)B_2H can be generated by breaking the B(2)−Co(5) and B(2)−B(1) interactions and bending the B(2) atom out, around and underneath a rectangular face (Chart 2c), to re-form the B(2)−B(1) interaction and two long B(2)−Co(2) and B(2)−Co(3) interactions (Chart 2d). With the exception of the Co(1)−Co(4) distance, this model predicts the observed bimodal distribution of M−B and M−M distances, and as expected for a trigonal prism, the Co(4)−Co(3)−Co(5) angle is nearly a right angle (88.3(2)°). In contrast to the trigonal prismatic form (Chart 2b), this isomeric structure permits both reasonable B−B and Co−B interaction distances.

It is a measure of the uncommon character of this compound that there are other ways to accommodate the observed geometry with the available valence electrons. However, although the relationship of the geometry of the cluster with electron count gives valuable insight into the bonding, in such a complex system it is important to have information on where the electrons are. Thus, molecular orbital calculations have been carried out to explore in more detail the electronic structure of $Co_5(CO)_{13}(\mu$-CO)B_2H in order to provide a closer look at the bonding.

MO Analysis. As stated above, the core structure of $Co_5(CO)_{13}(\mu$-CO)B_2H can be described as a *closo* Co_4B_2 octahedron, of which a Co_2B triangular face is capped by a $Co(CO)_3$ fragment. Application of the Wade−Mingos electron-counting rules[15] leads to an expected pec of 78 or 7 skeletal electron pairs (sep) for such a compound. Consequently, with a pec of 80 (or 8 sep's) $Co_5(CO)_{13}(\mu$-CO)B_2H can be considered as a new member belonging to the family of "rule-breaker" *closo* octahedral M_4E_2 (M = transition metal and E = main group atom) clusters. J.-F.H. has previously rationalized the electronic structure of this class of electron-rich compounds. For the sake of understanding, we briefly summarize the main results of these previous studies before addressing the bonding analysis of $Co_5(CO)_{13}(\mu$-CO)B_2H.[38−41]

Chart 2

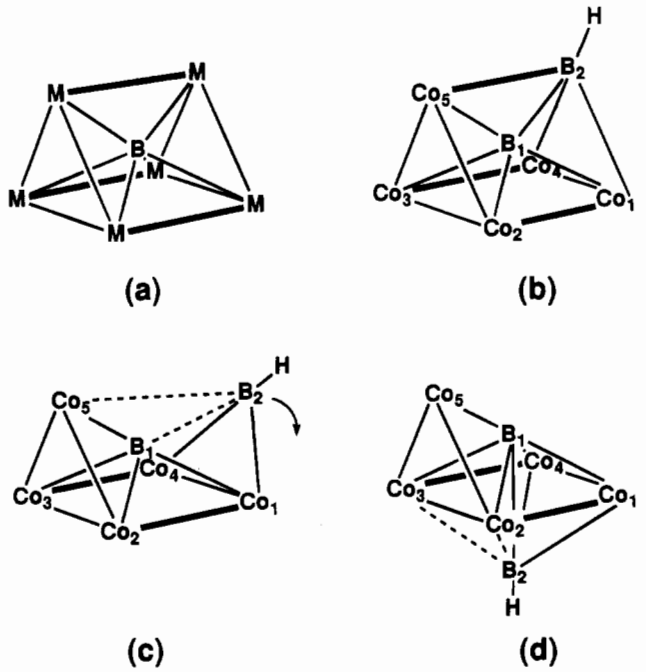

The pec generally adopted by the *closo* octahedral M_4E_2 compounds is either 66 (7 sep's), or 68 (8 sep's). The former obeys the Wade−Mingos rules, while the latter corresponds to the occupation of an extra skeletal MO, which is weakly metal−metal π-antibonding.[38] This MO is exclusively localized on the metallic square and lies in the middle of a large energy gap. Consequently, its occupation is strongly dependent on the electronegativity of the metal atoms, as exemplified by $Fe_4(CO)_{11}(\mu_4$-p-Tol))$_2$ (pec of 66)[42] and $Co_4(CO)_{10}(\mu_4$-PPh)$_2$ (pec of 68).[43] In these compounds, the difference in the covalent radii of M and E leads to a rather short contact (particularly for E belonging to the second period of the periodic table[44]) between the two E atoms capping the metallic square. This E···E separation, which is generally 12−20% longer than the one expected for a single bond, is observed because the corresponding electronic interaction is significantly bonding, regardless of the pec (66 or 68).[38−41]

We can envision the formation of $Co_5(CO)_{13}(\mu$-CO)B_2H (see the Experimental Section for details) by the interaction of the frontier molecular orbitals (FMO) of the *closo* octahedral

(31) Rath, N. P.; Fehlner, T. P. *J. Am. Chem. Soc.* **1988**, *110*, 5345.
(32) Khattar, R.; Fehlner, T. P.; Czech, P. T. *New J. Chem.* **1991**, *15*, 705.
(33) Fehlner, T. P.; Housecroft, C. E.; Scheidt, W. R.; Wong, K. S. *Organometallics* **1983**, 2, 825.
(34) *The Chemistry of Metal Cluster Complexes*; Shriver, D. F., Kaesz, H. D., Adams, R. D., Eds.; VCH: New York, 1990.
(35) Wade, K. *Adv. Inorg. Chem. Radiochem.* **1976**, *18*, 1.
(36) Mingos, D. M. P. *Acc. Chem. Res.* **1984**, *17*, 311−319.
(37) Housecroft, C. E.; Matthews, D. M.; Rheingold, A. L.; Song, X. *J. Chem. Soc., Chem. Comm.* **1992**, 842.
(38) Halet, J.-F.; Hoffmann, R.; Saillard, J.-Y. *Inorg. Chem.* **1985**, *24*, 1695.
(39) Halet, J.-F.; Saillard, J.-Y. *New J. Chem.* **1987**, *11*, 315.
(40) Albright, T. A.; Ae Yee, K.; Saillard, J.-Y.; Kahlal, S.; Halet, J.-F.; Leigh, J. S.; Whitmire, K. H. *Inorg. Chem.* **1991**, *30*, 1179.
(41) Kahlal, S.; Halet, J.-F.; Saillard, J.-Y. *Inorg. Chem.* **1991**, *30*, 2567.
(42) Vahrenkamp, H.; Walter, D. *Organometallics* **1982**, *1*, 874.
(43) Lower, L. D.; Dahl, L. F. *J. Am. Chem. Soc.* **1976**, *98*, 5046.
(44) Hansert, B.; Powell, A. K.; Vahrenkamp, H. *Chem. Ber.* **1991**, *124*, 2697.

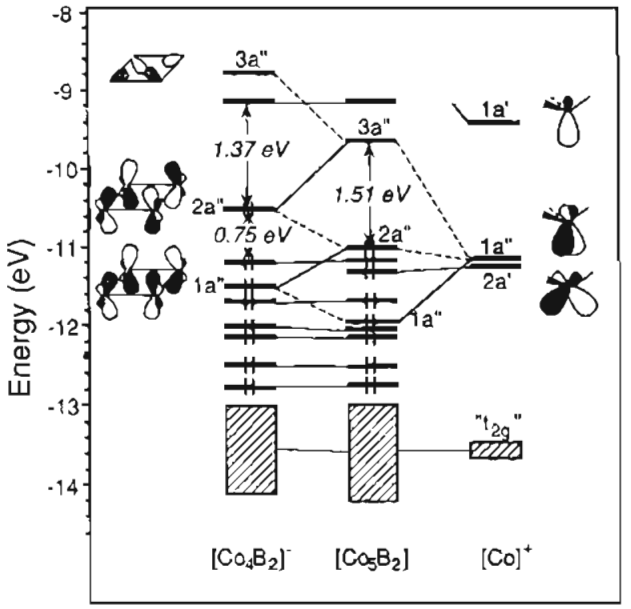

Figure 3. MO diagram of the model $Co_5(CO)_{13}B_2H$ from the interaction of the $[Co_4(CO)_{11}B_2H]^-$ (left) and $[Co(CO)_3]^+$ (right) fragments. The levels are labeled in the C_s symmetry group. The contribution of boron atoms in the sketched 1a″and 3a″ MO's are omitted for clarity.

fragment $[Co_4(CO)_{10}(\mu_4\text{-}B_2H)]^{2-}$ with the well-known FMO's of the capping unit $[Co(CO)_3]^{2+}$, as shown in Figure 3. As expected, a situation analogous to that of M_4E_2 clusters[38] is computed for the 8-sep octahedral fragment $[Co_4(CO)_{10}(\mu_4\text{-}CO)(B_2H)]$. Above a nest of 7 occupied skeletal MO's, a metallic nonbonding MO (2a″), in which two extra electrons can be housed, lies in the middle of a large energy gap.

The incoming $Co(CO)_3$ unit, which caps a triangular Co_2B face of the octahedral cluster, modifies somewhat the electronic structure of the Co_4B_2 core. Only one large HOMO−LUMO gap (1.51 eV) is now computed for the count of 8 sep's (or for a pec of 80), in agreement with the observed electron count, but not with the Wade−Mingos rules. The reason why the gap between the 8th and the 7th sep has disappeared in $Co_5(CO)_{13}(\mu\text{-}CO)B_2H$ is the following (see Figure 3). One component of the e set of the FMOs (1a″) of the $Co(CO)_3$ entity interacts strongly with the metallic nonbonding 2a″ MO of the octahedral Co_4B_2 fragment. To a first approximation, the result of this two-electron-two-orbital interaction is the destabilization of the 2a″ orbital and the stabilization of the 1a″ orbital. Consequently, the electron count of 8 sep's remains unchanged. The electron-rich nature of $Co_5(CO)_{13}(\mu\text{-}CO)B_2H$ is mainly due to the particular electronegative character of the atoms constituting the metallic square of the capped octahedral Co_5B_2 core. The 3a″ LUMO, which is mainly localized (61%) on the metallic triangular face (Co(2)−Co(3)−Co(5)) and to a lesser extent on B(1) (4%), is strongly metal−metal antibonding. The 2a″ HOMO, which possesses an important Co(1,2) and Co(5) contribution (46% and 11%, respectively), is slightly metal−metal antibonding.

From these results we suspect that the loss of a CO ligand should not be facile or should lead to a structural rearrangement of the Co_4B_2 core.

Where are the electrons? Calculations on $Co_5(CO)_{13}(\mu\text{-}CO)B_2H$ (idealized somewhat; see the Experimental Section) indicate some electron transfer from the boron atoms toward the metal atoms (see Table 3). The capping Co atom is almost neutral, while the Co atoms forming the metallic square are slightly negative. B(1), which is attached to Co(5), is slightly more positive than B(2). The electron-counting procedure used here does not require any through-space B···B bonding in $Co_5(CO)_{13}(\mu\text{-}CO)B_2H$. Nevertheless, a rather strongly positive overlap population (0.41) is computed, reflecting a significant attractive interaction between B(1) and B(2). This is partly due to the σ^*(B−B) FMO, which is sufficiently high in energy to avoid being importantly populated in $Co_5(CO)_{13}(\mu\text{-}CO)B_2H$.[38] Consequently, both size and electronic factors contribute to the very short boron−boron contact in $Co_5(CO)_{13}(\mu\text{-}CO)B_2H$ (ca. 10% longer than a single B−B bond[45]).

Table 3. EH Characteristics Computed for $Co_5(CO)_{13}(\mu\text{-}CO)B_2H$[a]

overlap populations		atomic net charges	
Co(1)−Co(2)[2.65 Å]	0.079	Co(1)	−0.162
Co(1)−Co(4)[2.65 Å]	0.116	Co(2)	−0.064
Co(2)−Co(3)[2.65 Å]	0.075	Co(5)	+0.006
Co(1)−B(1)[2.09 Å]	0.337	B(1)	+0.504
Co(1)−B(2)[2.09 Å]	0.310	B(2)	+0.401
Co(2)−B(1)[2.09 Å]	0.232		
Co(2)−B(2)[2.09 Å]	0.256		
Co(5)−B(1)[1.99 Å]	0.459		
B(1)−B(2)[1.85 Å]	0.410		

[a] The structure of $Co_5(CO)_{13}(\mu\text{-}CO)B_2H$ has been idealized (C_s symmetry) for the computations. Atomic separations are given in brackets.

As shown in Table 3, the different Co−B overlap populations computed for the idealized structure of $Co_5(CO)_{13}(\mu\text{-}CO)B_2H$ suggest an asymmetrical bridging of the boron atoms above and below the metallic square, with some lengthening of the bonds between B(2) and Co(2) and Co(3) and some shortening of the bonds between B(1) and Co(1) and Co(4) as observed experimentally. Indeed, this phenomenon such that each group of two M−E distances are shorter than the other two is sometimes observed in M_4E_2 compounds, in which the metal atoms depict a trapezoidal framework, of which one edge is bridged by a CO ligand. $Ru_4(CO)_{10}(\mu_4\text{-}PPh)_2$ provides a nice example.[46] We think that the asymmetry in the Co−B bonds is reinforced in $Co_5(CO)_{13}(\mu\text{-}CO)B_2H$ due to the additional capping Co(5) center.

This asymmetrical bridging of the boron atoms is in agreement with the alternative way to describe $Co_5(CO)_{13}(\mu\text{-}CO)B_2H$ as a skeletal isomeric form of the 80-electron Co_5B_2 trigonal prism (see above; Chart 2b), in which one short Co−B separation would be replaced by two long Co···B contacts (Chart 2d). Because of the difference in size between cobalt and boron, it turns out that the trigonal prismatic form is unlikely (difficulty to match reasonable B−B and Co−B bonding contacts), and as stated above, the capped octahedral geometry (Chart 2d) allows both B−B and Co−B interaction separations.

Origin of the Cobaltaboranes. Although a mixture of boron-containing products was obtained with either hexane or toluene as the solvent, very different results were obtained with SEt_2. Addition of SEt_2 to solid $Co_2(CO)_8$ caused CO evolution, but if it was rapidly followed by a less than stoichiometric amount of neat $BH_2{\cdot}SMe_2$ at 50 °C, a single boron-containing product was observed by NMR (^{11}B, SEt_2, 22 °C, $\delta = -15.7$, t, $J_{BH} = 120$ Hz; ^{1}H, toluene-d_8, 22 °C, $\delta = 3.25$, br q, $J_{BH} = 120$ Hz) with an estimated yield of 90%. Fractional crystallization at −40 °C removed most of the $Co_4(CO)_{12}$ and some other minor non-boron-containing products. The mass spectrum (EI) exhibits ions provisionally identified as $[(SMe_2)(CO)CoBH_2]^+$ and $[(SMe_2)CoBH_2]^+$. These data suggest the formation $(SR_2)_y(CO)_{4-x}CoBH_2{\cdot}SMe_2$ (R = Me, Et), compounds

(45) Wade, K. *New Scientist* **1974**, *62*, 615.
(46) Field, J. S.; Haines, R. J.; Smit, D. N. *J. Organomet. Chem.* **1982**, *224*, C49.

Scheme 1

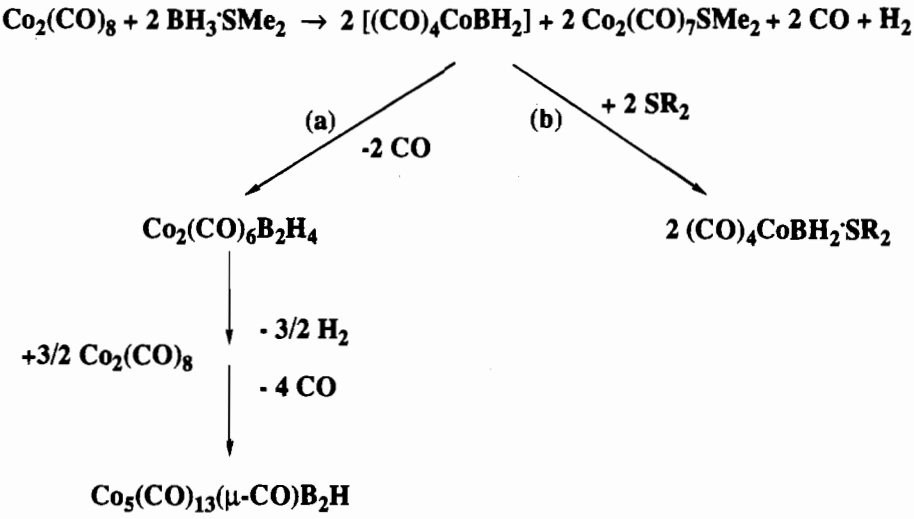

analogous to $(CO)_4CoBH_2$·THF. The reaction of $(SR_2)CoBH_2$·SMe_2 in hexane at 70 °C with or without additional $Co_2(CO)_8$ did not lead to the formation of $Co_2(CO)_6B_2H_4$, nor did it lead to decomposition.

If the reaction is carried out in the mixed solvent 50% SEt_2–50% hexane, evidence for the formation of higher nuclearity cobaltaboranes (see above) is found in the ^{11}B NMR spectrum. Therefore, $(SMe_2)_x(CO)_{4-x}CoBH_2$·$SMe_2$ and the other cobaltaboranes are formed via a pair of parallel reactions either from the reactants directly or from a common intermediate. The importance of the role of SR_2 in the course of the reaction is clear.

$Co_2(CO)_8$ undergoes ready substitution ($t_{1/2}$ for $AsPh_3$ at 25 °C is 30 s),[47] and the addition of SR_2 alone to $Co_2(CO)_8$ leads to the rapid evolution of CO and, presumably, the formation of $Co_2(CO)_7SR_2$. As, at 70 °C, BH_3·SMe_2 is partially dissociated, the $Co_2(CO)_8$ not only reacts with the B–H bond but can also react with the free SMe_2. Thus, we suggest the mechanism in Scheme 1 in which base-free $(CO)_4CoBH_2$ is formed as an intermediate at low concentration. It then dimerizes in the absence of excess SR_2 (path a—hydrocarbon solvent) or is trapped in the presence of SR_2 (path b—SR_2 solvent). For simplicity we have ignored the formation of $Co_4(CO)_{12}$ and the apparent extensive substitution of CO on cobalt that occurs when SR_2 is used as a solvent. Subsequent reaction of the B–H bonds of $Co_2(CO)_6B_2H_4$ with $Co_2(CO)_8$ would lead to the intermediate cobaltaboranes (not isolated) and, ultimately, to $Co_5(CO)_{13}(\mu$-$CO)B_2H$. The essence of the cluster building process is

$$B-H + Co-Co \rightarrow B-Co + Co-H \quad (3)$$

$$Co-H \rightarrow {}^1/_2Co-Co + {}^1/_2H-H \quad (4)$$

namely a σ-bond metathesis reaction of the B–H bond.

The reaction of BH_3·THF with $Co_2(CO)_8$ in THF produces $(CO)_4CoBH_2$·THF at −10 °C whereas BH_3·SMe_2 only reacts at 70 °C. This shows that the activity of the B–H bond in reaction 3 depends on the nature of the coordinated base in BH_3·L. It is well-known that the properties of the B–H bond do indeed depend on L.[48] Thus, the complexity of this chemistry depends in part on the ability of the base to (a) activate the B–H bond, (b) substitute for CO on Co, (c) trap the cobalt–borane intermediate, or (d) in the case of THF, be cleaved by the cobalt–borane product.

Acknowledgment. The support of National Science Foundation is gratefully acknowledged.

IC941288U

(47) Absi-Halabi, M.; Atwood, J. D.; Forbus, N. P.; Brown, T. L. *J. Am. Chem. Soc.* **1980**, *102*, 6248.

(48) Burg, A. B. In *Boron Chemistry-4*; Parry, R. W., Kodoma, G., Eds.; Pergamon: New York, 1980; p 153.